Optical Materials 49 (2015) 286–291

Contents lists available at ScienceDirect

Optical Materials

journal homepage: www.elsevier.com/locate/optmat

High efficiency and stable-yellow phosphorescence from OLEDs with a novel fluorinated heteroleptic iridium complex

Yan-Li Lv [a], Yong-Xu Hu [a], Jin-Hui Zhao [a], Guang-Wei Zhao [a], Ying Qi [a], Xiao Li [a,*], Hai-Jun Chi [a], Yan Dong [a], Guo-Yong Xiao [a], Zi-Sheng Su [b,*]

[a] School of Chemical Engineering, University of Science and Technology Liaoning (USTL), Anshan 114051, People's Republic of China
[b] State Key Laboratory of Luminescence and Applications, Changchun Institute of Optics, Fine Mechanics and Physics (CIOMP), Chinese Academy of Sciences, Changchun 130033, People's Republic of China

ARTICLE INFO

Article history:
Received 24 July 2015
Received in revised form 7 September 2015
Accepted 22 September 2015
Available online 30 September 2015

Keywords:
Optical material
Iridium complex
Electroluminescence
2-Phenylbenzo[*d*]thiazole
Phosphorescence
OLEDs

ABSTRACT

The performance of a heteroleptic *bis*-cyclometalated iridium complex based on 2-(2,3,4-trifluorophenyl) benzo[*d*]thiazole [$(tfbt)_2Ir(acac)$] was investigated as a new phosphorescent emitter in OLEDs. The devices showed very high efficiency at various dopant concentrations and maximum efficiency was achieved at 6 wt% dopant concentration. A comparison of the performances of phosphorescent OLEDs with the new emitter versus those with prototype-based $(bt)_2Ir(acac)$ emitter revealed a remarkable improvement of efficiency at all dopant concentrations. These preliminary results obtained with the tfbt-based emitter indicate that this family of cyclometalated ligands with multi-fluorine functionalization is a promising compound for the development of highly emissive complexes.

1. Introduction

Phosphorescent materials based on transition-metal complexes [1–5] have been extensively used to fabricate highly efficient organic light-emitting diodes (OLEDs) due to the whole utilization of the singlet and triplet excitons since the early phosphorescent materials were reported by Ma and Forrest et al. [6,7]. Among the phosphorescent materials, iridium(III) [Ir(III)] complexes are considered to be the most promising because they exhibit flourishing merits: (i) high phosphorescent quantum efficiency, (ii) good thermal stabilities, (iii) facile color tuning, (iv) flexible structural modifications. Those characteristic features of Ir(III) complexes are attributed to the efficient spin–orbit coupling from the Ir metal as well as the strong structural/electronic interactions between the Ir core and ligands. Besides preliminary red, green, and blue phosphorescent materials, yellow/orange phosphorescent materials which are used to fabricate simple two-element white OLEDs are also drawing more attention [8–11]. Therefore, high performance yellow/orange phosphorescent OLEDs are urgently desired. To obtain high performance phosphorescent devices, this type of phosphorescent emitters is crucial.

2-Phenylbenzothiazole (bt) is a prevalent ligand framework to construct typical yellow bis(2-phenylbenzothiozolato-$N,C^{2'}$)iridium(acetylacetonate) [$(bt)_2Ir(acac)$] complexes. As for as Ir–bt type complex is concerned, its emission wavelength, phosphorescent quantum yield, phosphorescent lifetime and so on are easily adjusted by structure modification. For example, Lu and Li et al. [12,13] reported that fine tuning of emission color of Ir(III) complexes from yellow to red via substituent effect on bt ligand. Our group demonstrated efficient red phosphorescent OLEDs based on Ir–bt type complex by elongating conjugate system with the alkenyl group [14]. Moreover, some functionalized groups such as carbazole and arylamine were introduced into bt ligand to successfully increase phosphorescent quantum yield of corresponding Ir(III) complexes and further improve device's efficiency [15–19]. In comparison, a lot of fluorinated compounds used in OLEDs display prominent properties [20–25]. It's well known that involvement of C–F bond shows the following advantages: (i) to reduce the rate of radiationless deactivation and enhance the photoluminescence (PL) efficiency; (ii) to make the complex sublime better for thin film deposition; (iii) to reduce self-quenching of luminescence by altering the molecular packing; (iv) to sometimes enhance the electron mobility of the corresponding compound; (v) to modify the highest occupied molecular orbital and the lowest unoccupied molecular orbital (HOMO–LUMO) levels and

* Corresponding authors.
E-mail addresses: lixiao@ustl.edu.cn (X. Li), suzs@ciomp.ac.cn (Z.-S. Su).

http://dx.doi.org/10.1016/j.optmat.2015.09.031
0925-3467/

further allow the optimization of carrier injection and the tuning of luminescent color [26]. Therefore, further modification of Ir–bt type complex with fluorination seems to be a wise choice to obtain OLEDs with improved device performances although some fluorinated Ir–bt type complexes have been used as highly emissive dopants in OLEDs [27–31].

Here, a novel Ir–bt type complex with multi-fluorine functionalization, namely $(tfbt)_2Ir(acac)$ (tfbt = 2-(2,3,4-trifluorophenyl) benzo[*d*]thiazole; acac = acetylacetone), was designed, synthesized and characterized. The influence of fluorine atoms on the photophysical and electrochemical properties of $(tfbt)_2Ir(acac)$ complex was systematically investigated. High efficient yellow phosphorescent OLEDs with $(tfbt)_2Ir(acac)$ as a new emitter in the conventional device structure were fabricated. Interestingly, the OLEDs based on fluorinated Ir–bt type complex exhibited superior performance compared with the prototype-based $(bt)_2Ir(acac)$ doped device. To the best of our knowledge, these efficiencies were comparable to the highest ever reported yellow phosphorescent OLEDs [29,31–33].

2. Experimental

2.1. Reagents and physical measurements

Commercially available reagents and starting materials were used for synthesis of the Ir(III) complex without further purification. Solvents were purified and dried by standard procedures prior to use. NMR spectra were recorded on a Bruker AC 500 spectrometer with tetramethylsilane (TMS) as an internal reference. Mass spectroscopy (MS) was performed on AB SCIEX API 3200 spectrometer. The melting point (mp) was measured on WRS-2A numeral melting point instrument. UV–vis absorption and PL spectra of the Ir(III) complex in CH_2Cl_2 solution of 1.0×10^{-5} mol L^{-1} were completed on a PerkinElmer Lambda 900 spectrophotometer and LS 55 fluorescence spectrophotometer, respectively. Thermogravimetric analysis (TGA) was undertaken under nitrogen atmosphere at a heating rate of 10 °C min^{-1} on a PerkinElmer Diamond TG-DTA 6300 thermal analyzer. The luminescent lifetime of the Ir(III) complex in CH_2Cl_2 were detected by a system equipped with a TDS 3052 digital phosphor oscilloscope pulsed Nd:YAG laser with a Third-Harmonic-Generator (THG) 355 nm output. Cyclic voltammetry experiments were conducted using a CHI 660D electrochemical analyzer with a scan rate of 100 mV s^{-1}. All measurements were carried out at room temperature (RT) unless otherwise specified.

2.2. Synthesis of the Ir(III) complex

2.2.1. Synthesis of 2-(2,3,4-trifluorophenyl)benzo[d]thiazole

2,3,4-Trifluorobenzoic acid 0.97 g (5.5 mmol) and NMP 5 mL were charged into the flask, then stirred and heated up to completely dissolving under nitrogen. Subsequently, PCl_3 0.3 mL (1.8 mmol) was added and then reacted for 0.5 h, and cooled. 2-Aminothiophenol 0.63 g (5 mmol) was then added into the flask and reacted 3 h under 120 °C. Deionized water was added into the reaction mixture resulting in dark gray solid, and then adjust pH to 8 with ammonia and filtrated. Gray product was obtained by recrystallization with anhydrous ethanol. Yield: 30%. Mp: 153.7–155.0 °C. ^{1}H NMR (500 MHz, CD_2Cl_2, TMS): δ 8.24–8.20 (m, 1 H), 8.13 (d, *J* = 8.0 Hz, 1 H), 8.03 (d, *J* = 7.5 Hz, 1 H), 7.61–7.57 (m, 1 H), 7.52–7.48 (m, 1 H), 7.24–7.19 (m, 1 H); ^{13}C NMR (125 MHz, CD_2Cl_2, TMS): 166.91, 154.04, 140.48, 140.22, 135.15, 132.22, 129.05, 127.19, 126.52, 126.15, 125.45, 123.67, 123.15, 121.77, 120.38, 120.30, 109.83.

2.2.2. Synthesis of $(tfbt)_2Ir(acac)$

Under N_2 atmosphere, a mixture of tfbt 0.504 g (1.9 mmol), $IrCl_3{\cdot}3H_2O$ 0.352 g, (1 mmol), 2-ethoxyethanol and water (16 mL, 3:1, v/v) were heated to 110–120 °C for 24 h. Then the reaction mixture was cooled to RT and water was added. The orange dimer was obtained after vacuum filtration and drying.

A mixture of the above resulting dimer, acetylacetone (Hacac) 2.1 mL (2 mmol), sodium carbonate 0.53 g (5 mmol) and 2-ethoxyethanol 12 mL was heated to 110–120 °C for 24 h under N_2 atmosphere. After cooling the mixture to RT and the addition of water, the resulting precipitate was collected by vacuum filtration and drying. The orange product was obtained by column chromatography on silica gel using petroleum and ethyl acetate as eluents. Yield: 37%. ^{1}H NMR (500 MHz, $CDCl_3$, TMS): δ 7.96 (d, *J* = 7.5 Hz, 2 H), 7.90 (d, *J* = 8.0 Hz, 2 H), 7.461–7.42 (m, 2 H), 5.76–5.73 (t, 2 H), 5.09 (s, 1 H), 1.17 (s, 6 H); ^{13}C NMR (125 MHz, $CDCl_3$, TMS): 186.23, 149.23, 132.40, 132.36, 127.82, 125.85, 122.51, 119.79, 117.49, 117.37, 101.94, 28.19. MS (ESI): *m*/*z* 842.9 [M+Na].

2.3. Device fabrication and EL measurements

OLEDs were fabricated through vacuum deposition of the materials at about 3×10^{-4} Pa onto ITO-coated glass substrates with a sheet resistance of 25 Ω sq^{-1}. The ITO-coated substrates were routinely cleaned by ultrasonic treatment in solvent and then cleaned by exposure to a UV–ozone ambient. All organic layers were deposited in succession without breaking vacuum. The devices were prepared with the following structures of ITO/NPB (45 nm)/TCTA (6 nm)/CBP: x wt% $(tfbt)_2Ir(acac)$ (10 nm)/Bepp2 (35 nm)/LiF (1 nm)/Al, in which NPB [4,4′-bis[N-(1-naphthyl)-N-phenyl-amino]-biphenyl], TCTA [tris(4-(9H-carbazol-9-yl)phenyl)amine], CBP (4,4′-N,N′-dicarbazolebiphenyl), Bepp2 [bis(2-(2-hydroxyphenyl)-pyridine)beryllium)] were used as hole transporting layer, electron blocking layer, host, and electron transporting layer, respectively, and LiF/Al as the composite cathode. Deposition rates and thicknesses of the layers were monitored *in situ* using oscillating quartz monitors. EL spectra were measured with OPT-2000 spectrophotometer. The luminance–current–voltage (*L*–*I*–*V*) characteristics were measured with a Keithley model 2400 power supply combined with a ST-900M spot photometer. All measurements were carried out at RT under ambient conditions.

3. Results and discussion

3.1. Synthesis and characterization

The complex $(tfbt)_2Ir(acac)$ was synthesized by reaction of tfbt with $IrCl_3{\cdot}3H_2O$ involving two steps according to the procedure previously reported [34]. Subsequently, it was purified by column chromatography to reach the sufficient purity for usability in OLEDs. The synthetic pathway was depicted in Scheme 1. The ligand tfbt were smoothly synthesized by condensation reaction of 2-aminothiophenol with 2,3,4-trifluorobenzoic acid, and then purified via recrystallization with ethanol in moderate yield. The compounds tfbt and $(tfbt)_2$ Ir(acac) were evidenced by MS, ^{1}H NMR and ^{13}C NMR.

3.2. Photophysical properties

The UV–vis absorption and PL spectra of $(tfbt)_2Ir(acac)$ in CH_2Cl_2 are depicted in Fig. 1 and exhibit the typical features of most Ir(III) complexes. Notably, the highest energy bands at 250–370 nm was assigned to spin-allowed $^1\pi$–π^* transitions mostly localized on the cyclometalated tfbt ligand while the broad weak absorption bands

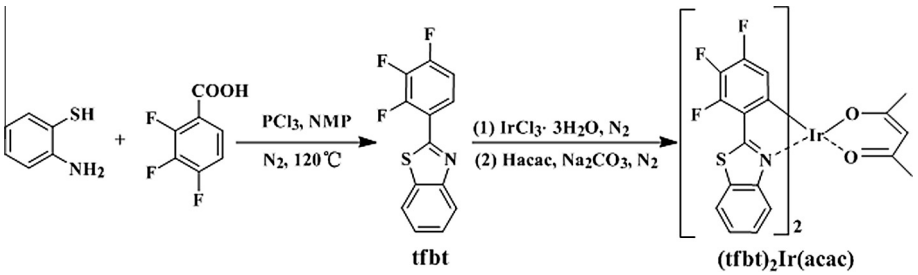

Scheme 1. The synthetic routes of complex $(tfbt)_2Ir(acac)$.

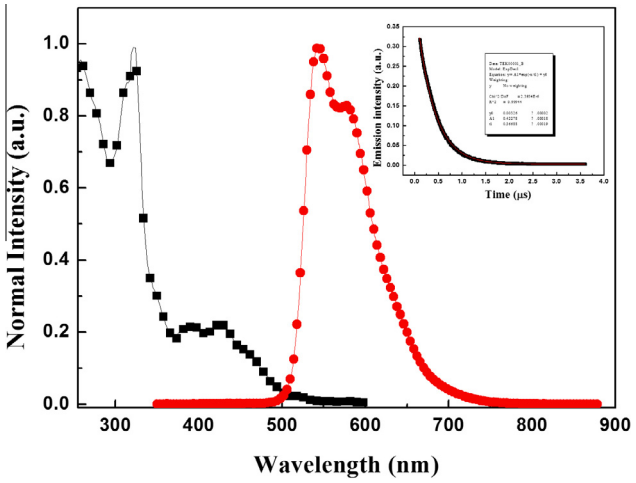

Fig. 1. UV–vis absorption and PL spectra of $(tfbt)_2Ir(acac)$ in CH_2Cl_2. Inset: the phosphorescent emissive lifetime curve of $(tfbt)_2Ir(acac)$ in degassed CH_2Cl_2.

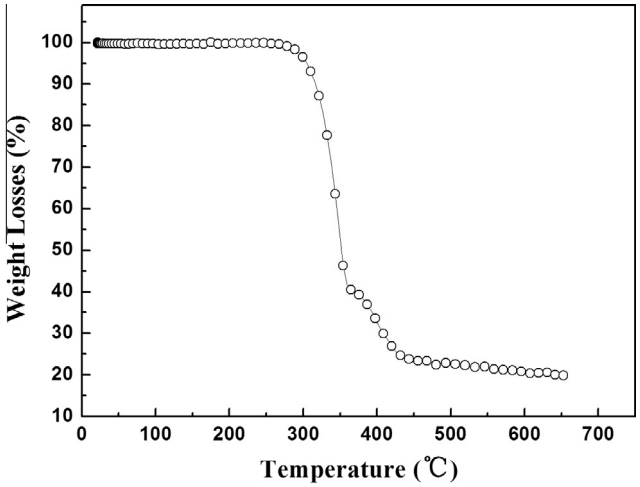

Fig. 2. TGA trace of $(tfbt)_2Ir(acac)$ measured at a heating rate of 10 °C min^{-1} under nitrogen atmosphere.

at 380–500 nm were attributed to an admixture of spin-allowed metal-to-ligand (^{1}MLCT) transition and spin-forbidden metal-to-ligand (^{3}MLCT) transition, respectively. When excited with 365 nm light, $(tfbt)_2Ir(acac)$ exhibited strong RT yellow phosphorescence with emission peak at 543 nm and shoulder peak at 578 nm, which could be assigned to predominantly ^{3}MLCT state radiative transitions. The emission quantum yields (φ_p) of $(tfbt)_2Ir(acac)$ in solution are determined as 0.56 with $(ppy)_2Ir(acac)$ (φ_p = 0.34) as reference. The φ_p value of $(tfbt)_2Ir(acac)$ is much higher than $(bt)_2Ir(acac)$ (φ_p = 0.26) [34], suggesting that the chemical modification of $(bt)_2Ir(acac)$ with multi-fluorine functionalization could greatly enhance the phosphorescence efficiency in solution.

The very short phosphorescent lifetime (τ_p) of $(tfbt)_2Ir(acac)$ in degassed CH_2Cl_2 at RT (inset of Fig. 1) is obtained with 0.37 μs, which is much shorter than those of popular $(ppy)_2Ir(acac)$ (ca. 1.6 μs) and $(bt)_2Ir(acac)$ (ca. 1.8 μs) [35].

The thermal stability of $(tfbt)_2Ir(acac)$ was evaluated by TGA under N_2 atmosphere with a scanning rate of 10 °C min^{-1}, as indicated in Fig. 2. Complex $(tfbt)_2Ir(acac)$ was thermally stable up to 305 °C with 5% weight loss, indicating that this Ir(III) complex showed excellent thermal stability which prevented the degradation of the emitting layer by current-induced Joule heat resulted from the operation of OLEDs.

3.3. Electrochemical properties

The electrochemical properties of $(tfbt)_2Ir(acac)$ was investigated by CV method in a three-electrode cell using ferrocene as the internal standard. HOMO and LUMO energy levels were estimated according to the electrochemical performance and UV–vis

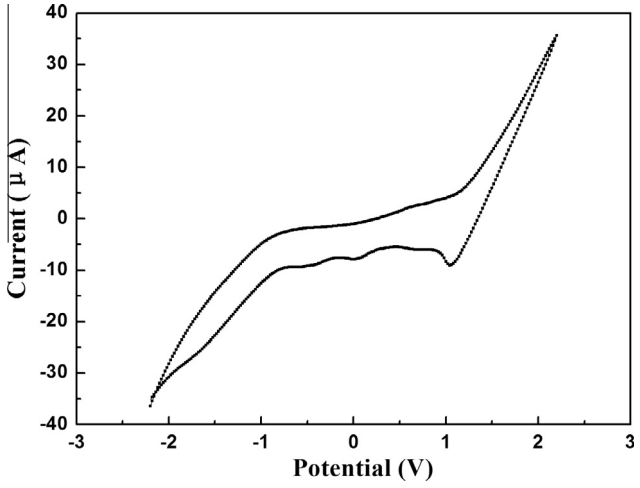

Fig. 3. CV curves of $(tfbt)_2Ir(acac)$ in CH_2Cl_2 with a scan rate of 100 mV s^{-1}.

absorption spectrum. As shown in Fig. 3, $(tfbt)_2Ir(acac)$ showed a reversible redox process over the anodic and cathodic range. The CV curves remained unchanged under multiple successive potential scans, suggesting its excellent stability against electrochemical oxidation and reduction. Complex $(tfbt)_2Ir(acac)$ exhibited the first oxidation potential with 1.50 V, and its HOMO energy level was calculated to be 5.80 eV relative to the value of 4.30 eV for ferrocene with respect to the zero vacuum level. Then LUMO energy level was obtained to be 3.37 eV from the HOMO energy level value and the absorption edge data. The HOMO and LUMO energy levels are summarized in Table 1.

Table 1
Photophysical, thermal and electrochemical characteristics of $(tfbt)_2Ir(acac)$.

Ir-complex	λ_{abs} (nm)	λ_{em} (nm)	φ_p	τ (μs)	T_d (°C)	HOMO (eV)	LUMO (eV)	E_g (eV)
$(tfbt)_2Ir(acac)$	320, 392, 430	542 (580)	0.56	0.37	305	5.80	3.37	2.43

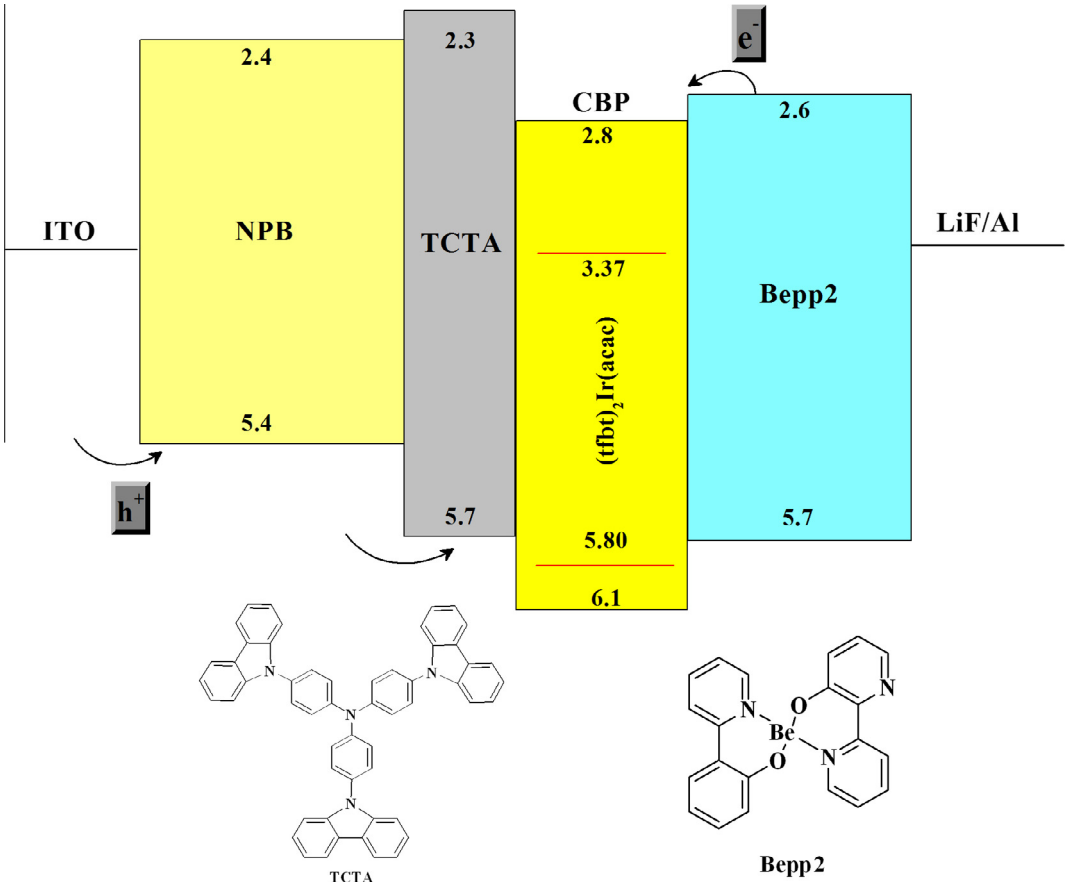

Fig. 4. Chemical structure of the different materials and energy levels of the yellow OLEDs investigated in this study.

3.4. Electrophosphorescent properties

In order to investigate the electrophosphorescent properties of $(tfbt)_2Ir(acac)$ as phosphor, devices with the structure of ITO/NPB (45 nm)/TCTA (6 nm)/CBP: x wt% $(tfbt)_2Ir(acac)$ (10 nm)/Bepp2 (35 nm)/LiF (1 nm)/Al were fabricated by high vacuum thermal evaporation on pre-cleaned ITO glass substrates as shown in Fig. 4. To determine the optimum doping concentration, four concentrations were investigated (2, 4, 6 and 9 wt%). The representative EL performance data of the triplet emitter are summarized in Table 2.

The EL spectra of $(tfbt)_2Ir(acac)$-doped devices under the voltage of 6 V are showed in Fig. 5. EL spectra of 6 wt% $(tfbt)_2Ir(acac)$-doped devices under the different voltage are also included in inset of Fig. 5. EL spectra showed a dominant yellow emission at 544 nm with the shoulder peak of 581 nm from $(tfbt)_2Ir(acac)$ without any other residual emission from host and/or adjacent layers, indicating effective energy transfer from the host to the dopant. Only inconspicuous emission from CBP was observed in the 6 wt% $(tfbt)_2Ir(acac)$-doped device under the low voltage. The EL spectra did not show any critical color shift with the doping concentrations and voltages, and the Commission International de L'Eclairage (CIE) coordinates (1931) remained almost constant at all concentrations (0.48, 0.50). The short triplet excited state lifetime of $(tfbt)_2Ir(acac)$ (ca. 0.37 μs) is beneficial to the remarkable color stability. The balance charge injection could also induce good color stability in the device.

The luminance–current–voltage (L–I–V) characteristics of $(tfbt)_2Ir(acac)$-doped devices are plotted in Fig. 6. All devices exhibited low turn-on voltages of ca. 3.0 V (defined as bias at a luminance of 1 cd m^{-2}). The device with 4 wt% $(tfbt)_2Ir(acac)$-doped concentration achieved the maximum luminance of 107,372 cd m^{-2} at the voltage of 10 V. Fig. 7 shows current efficiency–current density characteristics of the devices at various concentrations. The device efficiency varied with the doping concentration of $(tfbt)_2Ir(acac)$. The device with 6 wt% doping concentration exhibited a peak current efficiency of 60.3 cd A^{-1}, corresponding to the peak power efficiency of 47.3 lm W^{-1} at a current density of 1.0 mA cm^{-2}. At extremely high luminance of 10,000 cd m^{-2} (20.3 mA cm^{-2} and 5.9 V), the 6 wt% $(tfbt)_2Ir(acac)$-based device still possessed current efficiency of 49.3 cd A^{-1}, and power efficiency of 26.2 lm W^{-1}. To the best of our knowledge, these efficiencies were comparable to the highest ever reported yellow/orange phosphorescent OLEDs [29,31–33]. Based on the respective HOMO/LUMO levels of $(tfbt)_2Ir(acac)$, the host and the hole/electron-transporting layers (as shown in

Table 2
Summary of performances of the fabricated phosphorescent OLEDs.

Ir-complexes	Ratio (%)	$V_{turn\text{-}on}$ [a] (V)	λ_{EL} [b] (nm)	L_{max} [c] (cd m^{-2})	η_L [d] (cd A^{-1})	η_p [e] (lm W^{-1})
$(tfbt)_2Ir(acac)$	2	3.1	543 (581)	42,092	42.7	33.5
	4	3.1	544 (581)	107,372	54.8	43.0
	6	2.9	544 (581)	100,726	60.3	47.3
	9	2.9	543 (580)	84,628	50.7	38.8
$(bt)_2Ir(acac)$	4	4.5	558 (599)	34,800	40.7	21.3
	6	4.2	557 (600)	35,820	52.0	22.9
	9	4.3	557 (599)	31,800	42.9	19.1

[a] Turn-on voltage at a brightness of 1 cd m^{-2}.
[b] Maxium emission wavelength. Values in parentheses are shoulder peaks.
[c] Maximum luminance.
[d] Maximum current efficiency.
[e] Maximum power efficiency.

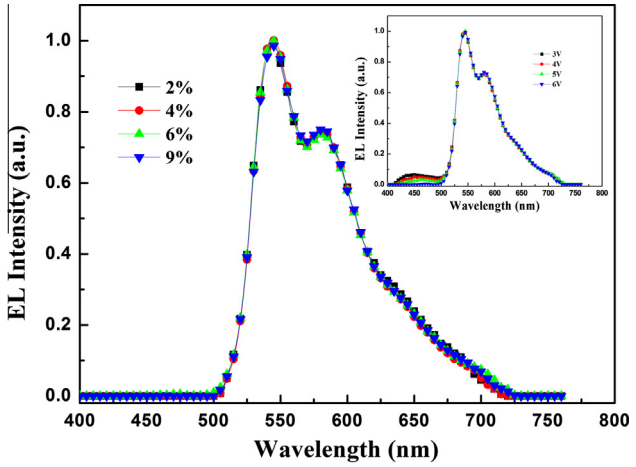

Fig. 5. EL spectra of $(tfbt)_2Ir(acac)$-doped devices under the voltage of 6 V. Inset: EL spectra of 6 wt% $(tfbt)_2Ir(acac)$-doped device under the different voltage.

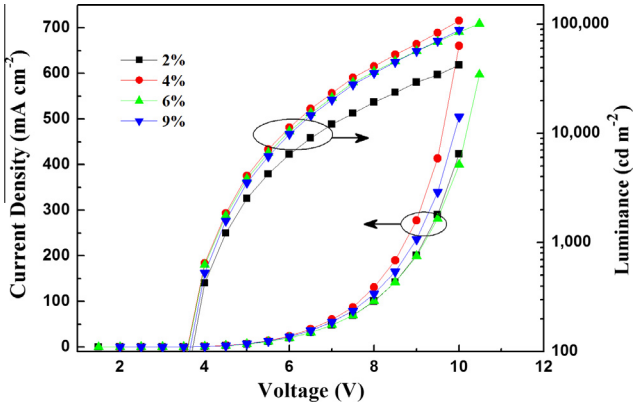

Fig. 6. *L–I–V* characteristics of $(tfbt)_2Ir(acac)$-doped devices.

Fig. 4), efficiency of phosphorescent OLEDs was assumed to result from the good hole/electron carrier-recombination balance in the phosphorescent OLEDs. The observable efficiency roll-off of about 40% at 100 mA cm^{-2} may be due to triplet–triplet annihilation and triplet–polaron annihilation [36,37].

To compare the performance of this new emitter $(tfbt)_2Ir(acac)$ with well known yellow dopants, a similar device was fabricated with the heteroleptic complex $(bt)_2Ir(acac)$ and tested in the same conditions. The $(bt)_2Ir(acac)$-doped device exhibited general efficiencies with a turn-on voltage of 2.9–3.1 V, a maximum current

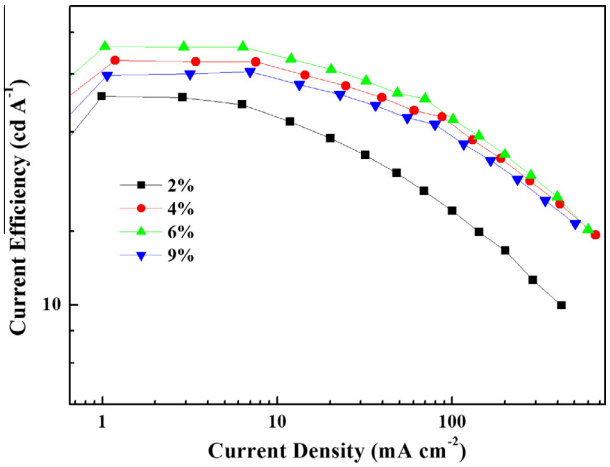

Fig. 7. Current efficiency–current density curves of $(tfbt)_2Ir(acac)$-doped devices.

efficiency of 52.0 cd A^{-1} and a peak power efficiency of 22.9 lm W^{-1} (see Table 2). The whole EL performances of the $(tfbt)_2Ir(acac)$-doped device greatly surpassed those of $(bt)_2Ir(acac)$-doped devices largely derived from excellent photophysical properties of $(tfbt)_2Ir(acac)$.

4. Conclusions

In conclusion, the performances of a heteroleptic *bis*-cyclometalated complex with 2-(2,3,4-trifluorophenyl)benzo[*d*]thiazole ligand as the new emitter in phosphorescent OLEDs had been investigated in detail. The devices showed very high efficiency at various dopant concentrations and maximum efficiencies (60.3 cd A^{-1} and 47.3 lm W^{-1}) had been achieved at 6 wt% dopant concentration. Stable yellow electrophosphorescence from the device was achieved due to short lifetime of $(tfbt)_2Ir(acac)$ and charge-injection balance. A comparison of the performances of phosphorescent OLEDs with the new emitter versus those of prototype-based $(bt)_2Ir(acac)$ emitter revealed a significant improvement of efficiency at all dopant concentrations. These preliminary results obtained with the tfbt-based emitter indicated that this family of cyclometalated ligand is promising for the development of highly emissive phosphorescent complexes.

Acknowledgements

Authors gratefully acknowledge the supports from the National Natural Science Foundation of China (Grant No. 61204021) and Talents training project of USTL (Grant No. 2014RC01).

References

[1] Y. Chi, P.-T. Chou, Chem. Soc. Rev. 39 (2010) 638–655.
[2] C. Fan, C.L. Yang, Chem. Soc. Rev. 43 (2014) 6439–6469.
[3] C.-L. Ho, W.-Y. Wong, Coord. Chem. Rev. 257 (2013) 1614–1649.
[4] M. Panigati, M. Mauro, D. Donghi, P. Mercandelli, P. Mussini, L. De Cola, G. D'Alfonso, Coord. Chem. Rev. 256 (2012) 1621–1643.
[5] Y. You, S.Y. Park, Dalton Trans. (2009) 1267–1282.
[6] Y.G. Ma, H.Y. Zhang, J.C. Shen, C.M. Che, Synth. Met. 94 (1998) 245–248.
[7] M.A. Baldo, D.F. O'Brian, Y. You, A. Shoustikov, S. Sibley, M.E. Thompson, S.R. Forrest, Nature 395 (1998) 151–154.
[8] S.-L. Lai, S.-L. Tao, M.-Y. Chan, M.-F. Lo, T.-W. Ng, S.-T. Lee, W.-M. Zhao, C.-S. Lee, J. Mater. Chem. 21 (2011) 4983–4988.
[9] T. Peng, Y. Yang, H. Bi, Y. Liu, Z. Hou, Y. Wang, J. Mater. Chem. 21 (2011) 3551–3553.
[10] P.-I. Shih, C.-F. Shu, Y.-L. Tung, Y. Chi, Appl. Phys. Lett. 88 (2006) 251110.
[11] P. Chen, W.F. Xie, J. Li, T. Guan, Y. Duan, Y. Zhao, S.Y. Liu, C.S. Ma, L.Y. Zhang, B. Li, Appl. Phys. Lett. 91 (2007) 023505.
[12] M. Li, H. Zeng, Y.-Y. Meng, H.-Q. Sun, S. Liu, Z.-Y. Lu, Y. Huang, X.M. Pu, Dalton Trans. 40 (2011) 7153–7164.
[13] J.Y. Li, R.J. Wang, R.X. Yang, W. Zhou, X. Wang, J. Mater. Chem. C 1 (2013) 4171–4179.
[14] G.Y. Xiao, P. Lei, H.J. Chi, Y.H. Lu, Y. Dong, Z.Z. Hu, Z.Q. Zhang, X. Li, Synth. Met. 159 (2009) 705–709.
[15] F. Xu, J.-Y. Kwon, J.-H. Kim, H.U. Kim, J.M. Lim, H. Cho, C. Lee, J. Lee, J.-I. Lee, D.-H. Hwang, Synth. Met. 162 (2012) 1421–1428.
[16] D. Liu, R.X. Yang, R.J. Wang, Dyes Pigm. 98 (2013) 317–322.
[17] X. Li, T.-N. Zang, H.-J. Chi, Y. Dong, G.-Y. Xiao, D.-Y. Zhang, Dyes Pigm. 106 (2014) 51–57.
[18] G.Y. Xiao, X. Li, H.J. Chi, Y.H. Lu, Y. Dong, Z.Z. Hu, J.L. Yu, M. Kimura, Synth. Met. 162 (2012) 497–502.
[19] X. Li, T.N. Zang, L.S. Yu, D.Y. Zhang, G.H. Lu, H.J. Chi, G.Y. Xiao, Y. Dong, Z. Cui, Z. Q. Zhang, Z.Z. Hu, Opt. Mater. 35 (2012) 300–306.
[20] V.V. Grushin, N. Herron, D.D. LeCloux, W.J. Marshall, V.A. Petrov, Y. Wang, Chem. Commun. 21 (2001) 1494–1495.
[21] J. Hu, G. Zhang, H.-H. Shih, P.i. Sun, C.-H. Cheng, Synth. Met. 158 (2008) 912–916.
[22] P.K. Koech, A.B. Padmaperuma, L. Wang, J.S. Swensen, E. Polikarpov, J.T. Darsell, J.E. Rainbolt, D.J. Gaspar, Chem. Mater. 22 (2010) 3926–3932.
[23] C. Wu, S. Tao, M. Chen, F.-L. Wong, Q. Yang, H.-W. Mo, W. Zhao, C.-S. Lee, Dyes Pigm. 96 (2013) 237–241.
[24] Q.-L. Xu, X. Liang, S. Zhang, Y.-M. Jing, X. Liu, G.-Z. Lu, Y.-X. Zheng, J.-L. Zuo, J. Mater. Chem. C 3 (2015) 3694–3701.
[25] Z. Li, Z. Wu, W. Fu, P. Liu, Bo Jiao, D. Wang, G. Zhou, X. Hou, J. Phys. Chem. C 116 (2012) 20504–20512.
[26] Y. Wang, N. Herron, V.V. Grushin, D. LeCloux, V. Petrov, Appl. Phys. Lett. 79 (2001) 449–451.
[27] W.-C. Chang, A.T. Hu, J.-P. Duan, D.K. Rayabarapu, C.-H. Cheng, J. Organomet. Chem. 689 (2004) 4882–4888.
[28] I.R. Laskar, T.-M. Chen, Chem. Mater. 16 (2004) 111–117.
[29] R.J. Wang, D. Liu, H.C. Ren, T. Zhang, H.M. Yin, G.Y. Liu, J.Y. Li, Adv. Mater. 23 (2011) 2823–2827.
[30] X.F. Yun, S.Z. Lin, X.T. Dong, Opt. Mater. 34 (2012) 1165–1170.
[31] C. Fan, L. Zhu, B. Jiang, Y. Li, F. Zhao, D. Ma, J. Qin, C. Yang, J. Phys. Chem. C 117 (2013) 19134–19141.
[32] J.-S. Lin, C.-N. Ku, P.-C. Huang, C.-A. Wu, M.-H. Chang, J.-L. Liou, M.-R. Tseng, Proc. SPIE 9183 (2014). 91831O (1–6).
[33] S. Zhang, Q.-L. Xu, J.-C. Xia, Y.-M. Jing, Y.-X. Zheng, J.-L. Zuo, New J. Chem. (2015), http://dx.doi.org/10.1039/c5nj00939a.
[34] M. Nonoyama, Bull. Chem. Soc. Jpn. 47 (1974) 767–768.
[35] S. Lamansky, P. Djurovich, D. Murphy, F. Abdel-Razzaq, H.-E. Lee, C. Adachi, P.E. Burrows, S.R. Forrest, M.E. Thompson, J. Am. Chem. Soc. 123 (2001) 4304–4312.
[36] M.A. Baldo, C. Adachi, S.R. Forrest, Phys. Rev. B 62 (2000) 10967.
[37] S. Reineke, K. Walzer, K. Leo, Phys. Rev. B 75 (2007) 125328.